

Online Real-time Multiple Spatiotemporal Action Localisation and Prediction

Gurkirt Singh¹ Suman Saha¹ Michael Sapienza²

Philip Torr² Fabio Cuzzolin¹

¹Oxford Brookes University ²Oxford University

{gurkirt.singh-2015, suman.saha-2014, fabio.cuzzolin}@brookes.ac.uk

{michael.sapienza, philip.torr}@eng.ox.ac.uk

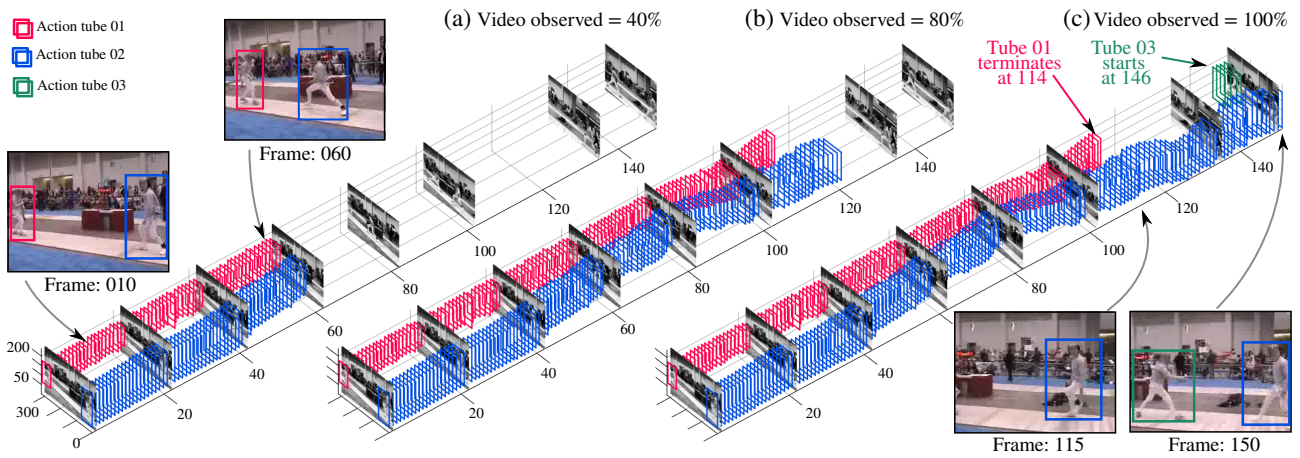


Figure 1: Online spatiotemporal action localisation in a test ‘fencing’ video from UCF-101 [39]. (a) to (c): A 3D volumetric view of the video showing detection boxes and selected frames. At any given time, a certain portion (%) of the entire video is observed by the system, and the detection boxes are linked up to incrementally build online space-time action tubes in real-time. Note that the proposed method is able to detect multiple co-occurring action instances (3 action instances are shown in different colours). Note also that one of the fencers moves out of the image boundaries between frames 114 and 145, to which our model responds by trimming action tube 01 at frame 114, and initiating a new tube (03) at frame 146.

Abstract

We present a method for multiple spatiotemporal (S/T) action localisation, classification and early prediction based on a single deep learning framework, able to perform in an online fashion and in real time. Our online action detection pipeline comprises of three main steps. In step one, two end-to-end trainable SSD (Single Shot MultiBox Detector) convolutional neural networks are employed to regress and classify detection boxes in each video frame potentially containing an action of interest, one from optical flow and one from RGB images. In step two, appearance and motion cues are combined by merging the detection boxes and classification scores generated by the two networks. In step three, sequences of detection boxes most likely to be associated with a single action instance, called action tubes, are

constructed incrementally and efficiently in an online fashion, allowing the system to perform early action class prediction and spatial localisation in real time. Empirical results on the challenging UCF101 and J-HMDB-21 datasets demonstrate new state-of-the-art results in S/T action localisation on UCF101, even when compared to offline competitors, and superior results on early action label prediction across the board. To the best of our knowledge, ours is the first real-time framework (up to 52fps) able to perform online spatio-temporal action localisation.

1. Introduction

Spatio-temporal human action localisation [49, 29, 25] in videos is inherently a challenging problem, and it becomes even harder if detection is to be performed in an on-

line setting at real-time speed. Current state-of-the-art action detectors [29, 25] are indeed far from working in real time and follow an ‘offline’ protocol in which information coming from the entire video (taken as a whole observable quantity) is used to detect and recognise action instances (particularly in the form of space-time ‘action tubes’ [6, 49], i.e., sequences of detection boxes related to a single action instance). In an online setting, by contrast, we need the system to construct action instance detections (e.g. to build action tubes) incrementally, on a frame-by-frame basis. In order for such a detector to be applied to real world problems such as surveillance, human robot interaction (e.g. surgical robotics) and other applications requiring a prompt response, streaming videos need to be processed in real time.

In this work, we design and demonstrate a deep learning framework able to perform spatial and temporal action localisation and classification in an online fashion (see Fig. 1) and in real-time, while further improving the detection accuracy of the latest state-of-the-art offline action detectors [29, 25] on the most complex available benchmark.

Current state of the art. With the rise of Convolutional Neural Networks (CNNs), impressive progress has been made in image classification [13] and object detection [5], motivating researchers to apply CNNs to action classification and localisation. Although the resulting state-of-the-art CNN-based action detectors [29, 6, 49] have achieved remarkable results, these methods are computationally expensive and their detection accuracy is still quite far from that of humans, limiting their real-world deployment. Most of these approaches [6, 49] are based on unsupervised region proposal algorithms [44, 57] and on an expensive multi-stage training strategy mutated from object detection [5]. For example, Gkioxari *et al.* [6] and Weinzaepfel *et al.* [49] both separately train a pair of (motion and appearance) CNNs and a battery of one-vs-rest Support Vector Machines (SVMs). This limits detection accuracy as each module is trained independently, yielding sub-optimal solutions.

The most recent efforts by Saha *et al.* [29] and Peng *et al.* [25] use a supervised region proposal generation approach [26] and eliminate the need of multi-stage training [5] by using a single end-to-end trainable CNN for action classification and bounding box regression. The results in [29, 25] showed that actionness scores produced by a supervised region proposal generation algorithm are crucial to improve detection accuracy. Although these approaches exhibit the best spatio-temporal action localisation accuracies to date, at test time, detection remains a two-step RPN [26] and RCNN [26] process, limiting real-time deployment. Furthermore, these methods’ mAP at high detection overlap values remain low, and incompatible with many real world applications.

Features of our framework. The online framework we propose takes advantage of the more recent SSD (Single

Shot MultiBox Detector) object detector [20] to address these issues with accuracy and speed. The SSD completely eliminates the region proposal generation step and is single-stage, end-to-end trainable. When combined with a novel, completely incremental multi-target tube generation algorithm, this leads to superior detection accuracy (compared to [49, 29, 25]) and real-time detection speed. Space-time action tubes [6, 29] are formed by linking SSD-generated frame-level detection windows over time, namely by looking at any time instant for associations between the set of current frame detection boxes and the existing action tubes. Unlike the methods in [6, 29, 25, 49], this is done in an online fashion as tubes are updated frame by frame, together with their overall action-specific scores.

When optical flow is computed in real time from the input RGB frames [14], the system achieves a test time detection speed of 30 fps (frames per second). If only appearance (RGB inputs) is considered, the framework performs at a remarkable 52 fps on a common machine with Intel Xeon CPU@2.80GHz (8 cores), and one NVIDIA Titan X GPU.

Recently, Soomro *et al.* [38] have proposed an approach able to predict the class label of an input test video and localise action instances within it by observing a relatively small portion of the entire video. This is referred to as early action prediction and localisation. They showed that both action prediction and online localisation accuracies improve over time as more and more video frames become available. Using Soomro *et al.* [38] as a baseline, we report here superior performances on both early action prediction and online action localisation on the temporally trimmed videos coming from J-HMDB-21, while maintaining a real-time detection speed. We go two steps further than Soomro *et al.* [38]. Firstly, we demonstrate action prediction and localisation capabilities from partially observed *untrimmed* streaming videos, on the challenging UCF101 dataset. Secondly, our framework runs in real-time, which is essential for real-world applications.

Overview of the approach. The proposed framework is outlined in Fig. 2. We train two SSD detection networks [20]: one on RGB frames (appearance), the other on optical-flow images [6]. At test time, the input to the framework is a sequence of RGB video frames (**a**). A real-time optical flow algorithm (**b**) [14] takes the RGB frames as input to produce flow images (**d**). As an option, (**c**) more accurate OF images can be computed in a non real-time setting [1] (but still incrementally). For each pipeline, the related detection network (**e**) takes as input an RGB (or OF) frame, and outputs a set of ‘regressed’ detection boxes (**f**), together with a set of class-specific confidence scores for each box indicating the likelihood of an action class being present there. We then merge (**g**) the class-specific confidence scores associated with the flow-based and the appearance-based detection boxes, as this significantly

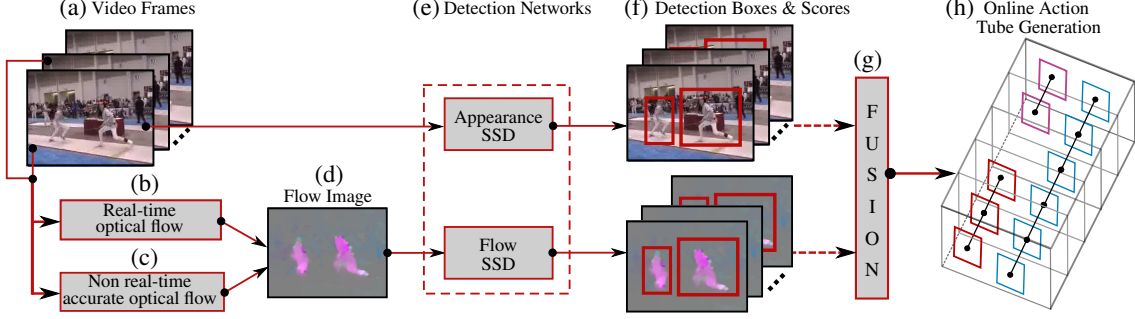


Figure 2. At test time, the input to the framework is a sequence of RGB video frames (a). A real-time optical flow (OF) algorithm (b) [14] takes the RGB frames as input to produce flow images (d). As an option, (c) a more accurate optical flow algorithm [1] can be used to incrementally process optical flow images (although not in real time). (e) RGB and OF images are fed to two separate SSD detection networks (§ 3.2). (f) Each network outputs a set of detection boxes along with their class-specific confidence scores (§ 3.2). (g) Appearance and flow detections are fused (§ 3.3). Finally (h), multiple action tubes are built up in an incremental, online fashion by associating current detections with partial tubes (§ 3.4).

boosts detection accuracy. Finally, sequences of detection boxes are linked up to form action-specific tubes in a completely online, incremental fashion (h).

Contributions. In summary, we present a holistic framework for the real-time, online spatial and temporal localisation of multiple action instances in videos which:

1. incorporates the newest SSD (Single Shot MultiBox Detector) [20] neural network architecture to simultaneously predict frame-level detection boxes and the associated action class-specific confidence scores, in a single-stage regression and classification approach (§ 3.2);
2. proposes an efficient algorithm capable of generating multiple action tubes incrementally (§ 3.4);
3. as a result, can provide early class label predictions and online spatio-temporal localisation results (Fig. 1) from partially observed action instances in untrimmed videos;
4. functions in real-time, while outperforming the previous (offline) state of the art on the challenging UCF101 dataset.

To the best of our knowledge, our framework is the first with a demonstrated ability to perform online spatial and temporal action localisation.

An extensive empirical evaluation on benchmarks demonstrates that our approach:

- is capable of superior early action prediction performance compared to the state of the art [38];
- significantly outperforms current offline methods using realistic detection thresholds greater than $\delta = 0.5$ (§ 4.2);
- achieves a real-time detection speed, that is 5 to 6 times faster than previous works (§ 4.4).

2. Related work

Deep learning architectures have been increasingly applied of late to action classification [11, 12, 33, 43], spatial

[6], temporal [32] and spatio-temporal [49] action localisation, and event detection [51].

Spatial action localisation is mostly addressed using segmentation [21, 37, 9] or region proposal and action-ness [6, 48]-based approaches. Supervoxel approaches [37] appear promising, but they require substantial computing time and resources, restricting their applications to offline settings. Gkioxari and Malik [6], in particular, have built on [5] and [33] to tackle spatial action localisation in temporally trimmed videos only, using Selective-Search region proposals, fine-tuned CNN features and a set of one-vs-rest SVMs.

Temporal action detection is mostly tackled using sliding window [18, 4, 42, 24, 47] approaches. The latter deliver good results [24, 4, 42], but they are too inefficient to work in real-time. The most recent efforts in this area are [32, 53, 52]. Recently, deep learning-based methods have made significant advances possible. For instance, Shou *et al.* [32] have employed the 3D CNNs [11, 43] to address temporal action detection in long videos. LSTMs are increasingly being used [52, 2, 34, 53] to address the problem. Dynamic programming has also been used to solve the problem efficiently [16, 3, 36]. Some of the above works [52, 2, 3, 52] can perform action detection in an online fashion. Unlike our framework, however, all these methods only address temporal, as opposed to spatial and temporal, detection.

Spatio-temporal action localisation can be approached in a supervised [25, 29], semi-supervised [45, 49], or weakly supervised [30, 50, 41] manner. Inspired by Oneata *et al.* [24] and Jain *et al.* [8], Gemert *et al.* [45] use unsupervised clustering to generate a small set of bounding box-like spatio-temporal action proposals. As their method is based on dense-trajectory features [46], it fails to detect actions characterised by small motions [45]. Weinzaepfel *et al.*'s work [49] performs both temporal and spatial detec-

tions by coupling frame-level EdgeBoxes [57] region proposals with a tracking-by-detection framework. However, temporal trimming is still achieved via a multi-scale sliding window over each track, making the approach inefficient for longer video sequences. More recently, Saha *et al.* [29] and Peng *et al.* [25] have made use of region proposal networks (RPNs) [26] to generate region proposal for actions, and solved the S/T association problem via Viterbi. Unlike our approach, however, these methods are not incremental, they rely on two separate stages for region proposal generation and classification, and suffer from slow network speed and heavy optical flow computation. In opposition, our framework employs a single shot SSD detector [20] and real-time optical flow algorithms [14], builds multiple action tubes in a fully incremental way, and works in real time.

Real-time methods. Relatively few efforts have been directed at simultaneous real time action detection and classification. Zhang *et al.* [56], for example, accelerate the two-stream CNN architecture of [33], performing action classification at 400 frames per second. Unlike our method, however, theirs cannot perform spatial localisation. Yu *et al.* [55] evaluate their real-time continuous action classification approach on the relatively simpler KTH [31] and UT-interaction [28] datasets. To the best of our knowledge, this is the first work to address real-time action localisation.

Online action prediction. Early, online action prediction has been studied using dynamic bag of words [27], structured SVMs [7], hierarchical representations [17], LSTMs and Fisher vectors [2]. Once again, unlike our framework, these approaches [27, 7, 17] do not perform online action localisation. Soomro *et al.* [38] recently proposed an online method which can predict an action’s label and location by observing a relatively smaller portion of the entire video sequence. However, they do not evaluate their approach (non real-time due to expensive segmentation) on untrimmed videos.

3. Methodology

Can be shortened or removed in an emergency. As outlined in Figure 2, our approach exploits an integrated detection network [20] (§ 3.2-Fig. 2e) to predict detection boxes and class-specific confidence scores for appearance and flow video frames independently. One of two alternative fusion strategies (§ 3.3-Fig. 2g) is then applied to fuse the cues extracted from appearance and flow-based detection networks. Finally, action tubes are built incrementally in an online fashion and in real time, using an efficient action tube generation algorithm (§ 3.4, Fig. 2h). This allows the system to generate early class label predictions (§ 3.5). All components are described in detail below.

3.1. Optical flow computation

The input to our framework is a sequence of RGB images. As in prior work in action localisation [29, 6, 49], we use a two-stream CNN approach [33] in which optical flow and appearance are processed in two parallel, distinct streams. As our aim is to perform action localisation in real-time, we employ real-time optical flow (Fig. 2b) [14] to generate the flow images (Fig. 2d).

As an option, one can compute optical flow more accurately (Fig. 2c), using the OpenCV¹ implementation by Brox *et al.* [1]. We train two different networks for the two OF algorithms, while at test time only one network is used depending on whether the focus is on speed rather than accuracy. Following the transfer learning approach on motion vectors of [56], we first train the SSD network on the accurate flow results, to later transfer the learned weights to initialise those of the real time optical flow network.

3.2. Integrated detection network

We use a single-stage convolutional neural network (Fig. 2(e)) for bounding box prediction and classification, which follows an end-to-end trainable architecture proposed in [20]. The architecture unifies a number of functionalities in single CNN which are, in other action and object detectors, performed by separate components [6, 49, 26, 29], namely: (i) region proposal generation, (ii) bounding box prediction and (iii) estimation of class-specific confidence scores for the predicted boxes. This allows for relatively faster training and much test time detection speeds.

Detection network design. For our integrated detection network we adopt the network design and architecture of the SSD [20] object detector, with an input image size of 300×300 . We would not use the 500×500 SSD architecture [20], as detection there is much slower [20]. As in [20], we use an ImageNet pretrained VGG16 network, and add an additional set of 5 convolutional layers on the top of the *Pool5* layer of VGG16, with randomly initialised weights. This gives us multiple feature maps at different scales, helping to cope with objects of different sizes. These multiple feature maps are then used to produce a fixed number of detection boxes with their classification scores. For each feature map small kernels are applied to produce either an action class score or a bounding box offset. For more details please refer to [20].

3.3. Fusion of appearance and flow cues

The detection boxes generated by the appearance and flow detection networks (Fig. 2f) need to be merged to improve robustness and accuracy (Fig. 2g). We conducted experiments using two fusion strategies.

Boost-fusion. Here we follow the approach in [29], with

¹<http://opencv.org/>

a minor modification. Firstly, we perform L-1 normalisation on the detection boxes' scores after fusion. Secondly, we retain any flow detection boxes for which an associated appearance based box was not found, as we found that discarding the boxes lowers the overall recall.

Fusion by taking the union-set. A different, effective fusion strategy consists in retaining the union $\{b_i^a\} \cup \{b_j^f\}$ of the two sets of appearance $\{b_i^a\}$ and flow $\{b_j^f\}$ detection boxes, respectively. The rationale is that in UCF-101, for instance, several action classes (such as 'Biking', 'IceDancing', or 'SalsaSpin') have concurrent action instances in the majority of video clips: an increased number of detection boxes may so help to localise concurrent action instances.

3.4. Online action tube generation

The output of our fusion stage (§ 3.3) is, for each video frame, a collection of detection boxes b , each endowed with a fused detection score $s_c(b)$ for class c . Detection boxes can be linked up in time to identify video regions likely to be associated with a single action instance, or 'action tube' [6].

We define an *action tube*² as a connected sequence of detection boxes in time, without interruptions, associated with a same action class c , starting and ending at arbitrary time points t_s, t_e in the video: $\mathcal{T}_c = \{b_{t_s}, \dots, b_{t_e}\}$.

Algorithm. The input to the algorithm are the frame-level detection boxes with their class specific scores. At each time step t , the top n class-specific detection boxes $\{b_c\}$ are selected by applying non-maximum suppression on a per-class basis. At the first frame of the video, $n_c(1) = n$ action tubes per class c are initialised using the n detection boxes at $t = 1$. The algorithm incrementally grows the tubes over time by adding one box at a time. The number of tubes $n_c(t)$ varies with time, as new tubes are added and/or old tubes are terminated. Note that, at each time step we sort the action tubes so that the best tube can claim the best box first. We perform the binary labelling $l \in \{c, 0\}$ for each tube at each time step after associating a box with a tube by using an online Viterbi algorithm. Action tubes are constructed by applying the following 7 steps at every new frame at time t :

1. Execute steps 2 to 7 for each class c .
2. Sort the action tubes generated up to $t - 1$ in decreasing order, based on the mean of the class scores of the tube's member detection boxes.
3. **LOOP START:** $i = 1$ to $n_c(t)$ - traverse the sorted tube list.
4. Pick tube \mathcal{T}_c^i from the list and find a matching box for it among the n class-specific detection boxes $\{b_c^j, j = 1, \dots, n\}$ at frame t based on the following conditions:

- (a) for all $j = 1, \dots, n$, if the IoU (Intersection over Union) between the last box of tube \mathcal{T}_c^i and the detection box b_c^j is greater than a threshold λ , then add it to a potential match list \mathcal{B}^i ;
 - (b) if the list of potential matches is not empty, $\mathcal{B}^i \neq \emptyset$, select the box b_c^{max} from \mathcal{B}^i with the highest score for class c as the match, and remove it from the set of available detection boxes at time t ;
 - (c) if $\mathcal{B}^i = \emptyset$, retain the tube anyway, without adding any new detection box, unless more than k frames have passed with no match found for it.
5. Update the temporal binary labelling for tube \mathcal{T}_c^i using the score $s(b_c^{max})$ of the selected box b_c^{max} (see next Paragraph).
 6. **LOOP END**
 7. If any detection box is left unassigned, start a new tube at time t using this box.

In all our experiments, we set $\lambda = 0.1$, $n = 10$, and $k = 5$.

Temporal labelling. Although n action tubes per class are initialised at frame $t = 1$, we want all action specific tubes to be allowed to start and end at any arbitrary time points t_s and t_e . The online temporal relabelling step 5. in the above algorithm is designed to take care of this.

Similarly to [29, 3], each detection box b_r , $r = 1, \dots, T$ in a tube \mathcal{T}_c , where T is the current duration of the tube and r is its temporal position within it, is assigned a binary label $l_r \in \{c, 0\}$, where c is the tube's class label and 0 denotes the background class. The temporal trimming of an action tube thus reduces to finding an optimal binary labelling $\mathbf{l} = \{l_1, \dots, l_T\}$ for all the constituting bounding boxes. This can be achieved by maximising the following energy for each tube \mathcal{T}_c :

$$E(\mathbf{l}) = \sum_{r=1}^T s_{l_r}(b_r) - \alpha_l \sum_{r=2}^T \psi_l(l_r, l_{r-1}), \quad (1)$$

where $s_{l_r}(b_r) = s_c(b_r)$ if $l_r = c$, $1 - s_c(b_r)$ if $l_r = 0$, α_l is a scalar parameter, and the pairwise potential ψ_l is defined as: $\psi_l(l_r, l_{r-1}) = 0$ if $l_r = l_{r-1}$, $\psi_l(l_r, l_{r-1}) = \alpha_c$ otherwise. The maximisation problem (1) can be solved by Viterbi dynamic programming [29].

Online Viterbi. An optimal labelling $\hat{\mathbf{l}}$ for a tube \mathcal{T}_c can be generated by a Viterbi backward pass at any arbitrary time instant t in linear time. We keep track of past edges from the start of the tube up to $t - 1$, which eliminates the requirement of an entire backward pass at each time step. This makes temporal labelling very efficient, and suitable to be used in an online fashion. This can be further optimised for much longer videos by finding the coalescence point [40]. As stated in step 5. above, the temporal labelling of each tube is updated at each time step whenever a new box is

²Action tubes remind us of 'tracklets' in multi-target tracking [23]. Compare the temporal association of human detections to generate multi-people tracks in [22, 35].

added. In the supplementary material, we present a pseudocode of our online action tube generation algorithm.

3.5. Early action prediction and localisation

As for each test video multiple tubes are built incrementally at each time step t (§3.4), we can predict at any time instant the label of the whole video as the label of the highest-scoring tube, where the score of a tube is defined as the mean of the tube boxes' individual detection scores:

$$\hat{c}(t) = \arg \max_c \left(\max_{\tau_c} \frac{1}{T} \sum_{r=1}^T s(b_r) \right). \quad (2)$$

4. Experiments

We test our online framework (§ 3) on two separate challenging problems: i) early action prediction (§ 4.1), ii) on-line spatio-temporal action localisation (§ 4.2), including a comparison to offline action detection methods. Evidence of real time capability is provided in (§ 4.4).

In all settings we generate results by running our framework in five different ‘modes’: 1) *Appearance (A)* – only RGB video frames are processed by a single SSD; 2) *Real-time flow (RTF)* – optical flow images are computed in real-time [14] and fed to a single SSD; 3) *A & RTF*: both RGB and real-time optical flow images are processed by a SSD in two separate streams; 4) *Accurate flow (AF)* optical flow images are computed as in [1], and 5) *A & AF*: both RGB and non real-time optical flow frames [1] are used.

Modes 1), 2) and 3) run in real-time whereas modes 4) and 5)'s performances are non real-time (while still working incrementally), due to the relatively higher computation time needed to generate accurate optical flow.

Datasets. We evaluate our model on the standard UCF-101 [39] and J-HMDB-21 [10] benchmark datasets. UCF-101 is the largest and one of the most diversified and challenging datasets. It contains realistic sequences with a large variation in camera motion, appearance, human pose, scale, viewpoint, clutter and illumination conditions. Although each video only contains a single action category, it may contain multiple action instances of the same action class, with different spatial and temporal boundaries. A subset of 24 classes out of 101 (‘split 1’) comes with spatio-temporal localisation annotation. As in [29, 54, 25, 49], we test our method on split 1.

J-HMDB-21 [10] is a subset of the HMDB-51 dataset [15] with 21 action categories and 928 videos, each containing a single action instance and trimmed to the action's duration.

Evaluation metrics. For the early action label prediction (§ 4.1) and the online action localisation (§ 4.2) tasks we follow the experimental setup of [38], and use the traditional localisation metrics AUC (area under the curve) and mAP (mean average precision). We report performance as

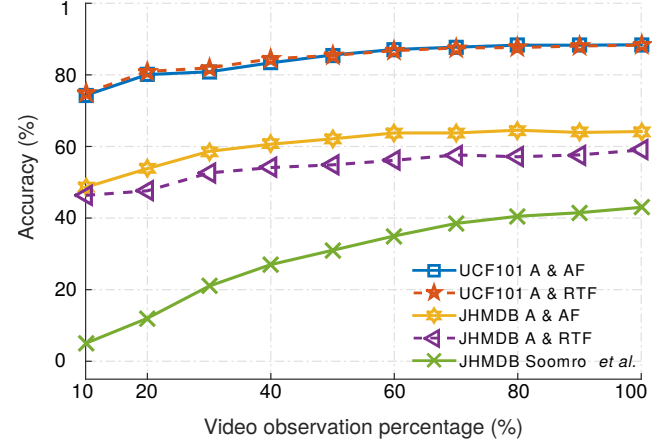


Figure 3. Early action label prediction results on the UCF101 and J-HMDB-21 datasets.

a function of *Video Observation Percentage*, i.e., with respect to the portion (%) of the entire video observed before predicting action label and location. We also report a performance comparison to offline methods using the protocol by Weinzaepfel *et al.* [49].

There are differently parsed version available of ST annotations for 24 classes of UCF101 dataset. We gathered these annotations from [29, 49, 45] correct multiple errors from these version by visually looking at suspicious videos. This new version of ST annotations is available at <https://github.com/gurkirt/corrected-UCF101-Annots>. We make use of these annotations in all of our experiments.

4.1. Early action label prediction

Although action tubes are computed by our framework frame by frame, we sample them at 10 different time ‘check-points’ along each video, starting at 10% of the total number of video frames and with a step size of 10%. At each check-point we label a video as per the label of the current tube with the best classification score (§ 3.5). We use the union-set and boost fusion strategies (§ 3.3) for UCF101 and J-HMDB-21, respectively.

Fig. 3 compares the early action prediction accuracy of our approach with that of [38], as a function of the portion (%) of video observed. Our method clearly demonstrates superior performance, as it is able to predict the actual video label by observing a very small portion of the entire video at a very initial stage. For instance, by observing only the initial 10% of the videos in J-HMDB-21, we are able to achieve a prediction accuracy of 48% as compared to 5% by Soomro *et al.* [38], which is in fact higher than the 43% accuracy achieved by [38] after observing the *entire* video.

Compared to [38] we take one step further, and perform early label prediction on the untrimmed videos of UCF101 as well (see Fig. 3). It can be noted that our method per-

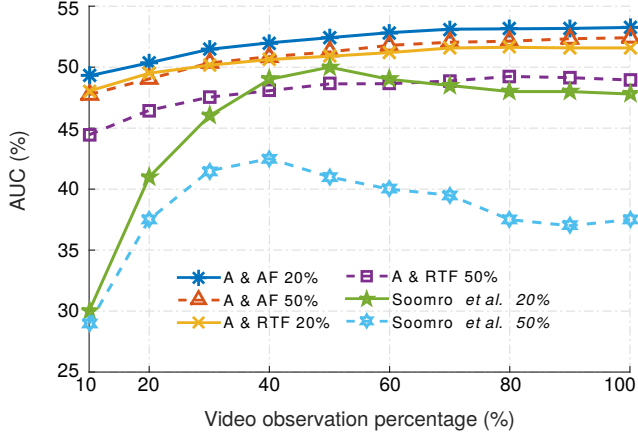


Figure 4. Online action localisation results using the AUC metric on J-HMDB-21, at IoU thresholds of $\delta = 20\%$, 50% .

forms much better on UCF101 than on J-HMDB-21 at the prediction task. This relatively higher performance may be attributed to the larger number of training examples, subject to more modes of variations, present in UCF101, which improves the generalisation ability of the model and prevents it from overfitting. Interestingly we observed that the performances of the real-time (A & RTF) and non real-time (A & AF) modalities are quite similar, which suggests either that accurate optical flow is not necessary for action detection on UCF101 dataset. It might be interesting to see the performance using more recent and accurate offline optical flow methods.

To the best of our knowledge, we are the first to report early action label prediction (and online action localisation, see § 4.2) results on the UCF101 dataset.

4.2. Online spatio-temporal action localisation

Performance over time. Our action tubes are built incrementally and carry associated labels and scores at each time step. At any arbitrary time t , we can thus compute the spatio-temporal IoU between the tubes generated by our online algorithm and the ground truth tubes, up to time t .

Fig. 4 plots the AUC curves against the observed portion of the video at different IoU thresholds ($\delta = 20\%$ and 50%) for the proposed approach versus our competitor [38]. Our method outperforms [38] on online action localisation by a large margin at all the IoU thresholds and video observation percentage. Notice that our online localisation performance (Fig. 4) is a stable function of the video observation percentage, whereas, Soomro *et al.* [38]’s method needs some ‘warm-up’ time to reach stability, and its accuracy slightly decreases at the end.

Note that Soomro *et al.* [38] only report online spatial localisation results on the temporally trimmed J-HMDB-21 test videos, and their approach lacks temporal detection capabilities. Our framework, instead, can perform online

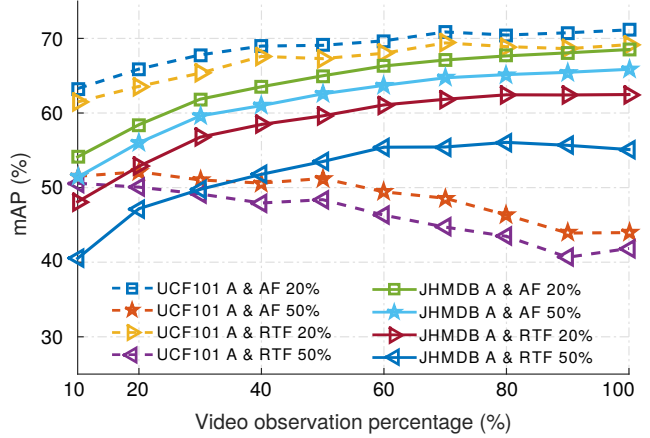


Figure 5. Action localisation results using the mAP metric on UCF101 and JHMDB-21, at IoU thresholds of $\delta = 20\%$, 50% .

spatio-temporal action localisation: to demonstrate this, we present results on the temporally untrimmed UCF101 test videos as well, shown in Fig. 5, where we used the mAP metric.

Interestingly, for UCF101, at a relatively smaller IoU threshold ($\delta = 20\%$) the performance gradually increases over time as more video frames are observed, whereas at a higher IoU threshold ($\delta = 50\%$) it slightly degrades over time. UCF101 videos are temporally untrimmed, most of action instances begin at the start of the video and finish much earlier than end of video. If the temporal labelling is not very accurate, which required at high thresholds ($\delta = 50\%$), this might result in more false positive as video progress, hence the drop in performance over time at $\delta = 50\%$.

Global performance. To demonstrate the strength of our online framework, we compare as well its absolute detection performances to those of the top offline competitors [29, 49, 25, 54]. To make a fair comparison with [29], we evaluate their offline tube generation method using detection bounding boxes produced by SSD network. Similar to [19], we report the mAP averaged over thresholds from 0.5 to 0.95 in steps of 0.05.

Results on UCF101 are reported in Table 1. In an online real-time setting we achieve an mAP of 67.34% compared to 66.55% reported by [29] at the standard IoU threshold of $\delta = 0.2$. In non-real time mode, we observe a further performance improvement of around 2%, leading to a 69.22% mAP.

It is important to observe the much higher gains we obtain at higher IoU thresholds, i.e., under more realistic requirements. For instance, we report gains of 7.7% at $\delta = 0.5$ and gain of 4% with mAP averaged over varied thresholds from 0.5 to 0.95, respectively. Note that in this case *union-set-fusion* significantly outperforms *boost-fusion*. As UCF-101 includes many co-occurring action in-

Table 1. S/T action localisation results (mAP) on UCF101 split1.

IoU threshold δ	0.2	0.5	0.75	0.5:0.95
Yu <i>et al.</i> [54] [†]	26.50	–	–	–
Weinzaepfel <i>et al.</i> [49] [†]	46.77	–	–	–
Peng and Schmid [25] [†]	42.67	–	–	–
Saha <i>et al.</i> [29]	66.55	36.37	07.94	14.37
Appearance (A)*	64.05	37.93	12.60	17.10
Real-time-flow (RTF)*	43.97	14.79	00.01	03.61
A & RTF (boost-fusion)*	66.29	40.00	10.74	16.89
A & RTF (union-set)*	67.67	39.94	11.05	17.21
Accurate - flow (AF)**	61.67	29.82	02.61	10.74
A & AF (boost-fusion)**	68.83	41.84	11.80	17.84
A & AF (union-set)**	69.13	42.39	11.50	18.17
Offline [29] A & AF (union-set)	69.22	40.42	08.78	16.98

* Real-time ** Non real-time

[†] These method does not use same annotation as ours or [29].

stances, we may infer that the former fusion strategy improves performance by providing a larger number of high confidence boxes from either appearance or flow network. When a single action is present in each video, as in JHMDB, *boost-fusion* seems to perform better (as we can observe in Table 2). We present a class-wise performance comparison of the two fusion strategies in the supplementary material.

Table 2 reports action detection results, averaged over the three splits of *J-HMDB-21*, and compares them with those to our closest (offline) competitors. Our framework outperforms the multi-stage approaches of [6, 48, 49] in non real-time mode at the standard IoU threshold of 0.5. It is not state-of-the art when compared to [29, 25], which both make use of a two-stage Faster RCNN architecture.

It is important to point out that [25] employs a battery of frame-level detectors, among which one based on strong priors on the human body parts. Our approach does not make any prior assumption on the object it detects, thus arguably more general-purpose. Still our approach is competitive with the best offline methods, while being online and real-time. Merging appearance and flow (A & AF) leads to an improvement of 2.11% at $\delta = 0.5$ over flow (AF) mode.

4.3. Discussion

The optical flow stream is an essential part of the framework that is needed to achieve high performance. It is clear from Table 1 and Table 2 that optical flow plays a much bigger role on the JHMDB dataset as compare to UCF101. For instance, at an IoU threshold of 0.5, the difference between appearance and optical flow mAP is +8.5% and −15% for UCF101 and JHMDB respectively. Similar trends were observed by [29] in their experiments.

We evaluate the offline tube generation method of [29] using the detection bounding boxes produced by the SSD network to make fair comparison and in order to understand what is influencing the performance. It is clear from Table 1 that our online tube generation performs better than the of-

Table 2. S/T Action localisation results (mAP) on J-HMDB-21.

IoU threshold δ	0.2	0.5	0.75	0.5:0.95
Gkioxari and Malik [6]	–	53.30	–	–
Wang <i>et al.</i> [48]	–	56.40	–	–
Weinzaepfel <i>et al.</i> [49]	63.10	60.70	–	–
Saha <i>et al.</i> [29]	72.63	71.50	43.30	40.03
Peng and Schmid [25]	74.10	73.10	–	–
Appearance (A)*	50.03	48.39	31.41	27.83
Real-time-flow (RTF)*	55.86	47.21	08.13	18.84
A & RTF (union-set)*	59.04	55.84	31.19	29.66
A & RTF (boost-fusion)*	62.57	54.16	08.38	21.02
Accurate - flow (AF)**	65.59	63.03	20.94	29.31
A & AF (union-set)**	66.28	64.38	29.29	32.39
A & AF (boost-fusion)**	69.07	66.52	21.15	30.66
Offline [29] A & AF (boost-fusion)	69.36	66.76	20.85	30.69

* Real-time ** Non real-time

fine tube generation of [29] on UCF101. The performance on JHMDB dataset (Table 2) is comparable. We can infer that the performance increase is coming from both the better boxes from the SSD network as well as the proposed online tube generation method. On the other hand, due to relatively smaller size of the JHMDB dataset, the trained SSD models might have reached to a overfitting state. Besides, cross validating CNNs hyper-parameters (e.g. learning rate), we might further improve the performance on JHMDB.

4.4. Test time detection speed

To support our claim to real time capability, we report the test time detection speed of our pipeline on UCF-101 under all three types of input (appearance, RGB + real time flow, RGB + accurate flow, Table 3). Numbers in Table 3) were generated using a desktop computer with an Intel Xeon CPU@2.80GHz (8 cores with hyper-threading) and a NVIDIA Titan X GPU. Appearance and flow detection boxes (§ 3.2) were extracted by running two processes in parallel on a single GPU. For action tube generation and trimming (§ 3.4) we ran 8 CPU threads in parallel.

Real-time capabilities can be achieved by either not using optical flow (RGB only) or by computing real-time optical flow [14] on a CPU in parallel with two CNN forward passes on a GPU with single frame latency. While processing the forward passes of detection networks at current time step, we compute optical flow for next time step on a CPU in parallel, which results in single frame latency. We use the real-time optical flow algorithm [14] in a customised setting, with minimum number of pyramid levels set to 2 instead of 3, and patch overlap 0.6 rather than 0.4. Optical flow computation averages around 6 ms per image, while gradient pyramid building and memory allocation take 10 ms and 1 ms each. The overall real-time optical flow image computation time averages around 17 ms.

To the best of our knowledge, we are the first to report test time detection speed for online spatio-temporal action

localisation. With final detection speed of 52 fps (when using only RGB frames) and 30 fps (when using also real time optical flow), our framework is able to detect multiple co-occurring action instances in real-time.

Table 3. Per frame test time detection speed.

Framework modules	RGB only	RGB + RTF	RGB + AF
Flow computation (ms*)	–	17.0	110
Detection network time (ms*)	17.1	29.3	29.2
Tube generation time (ms*)	1.2	1.5	1.5
Detection speed without latency (fps**)	52	20	7
Detection speed with latency (fps**)	52	30	9

* ms - milliseconds ** fps - frame per second.

5. Conclusions

We presented a novel online framework for action localisation and prediction able to address the challenges involved in concurrent multiple human action recognition, spatial localisation and temporal detection, in real time. Thanks to an efficient deep learning strategy for the simultaneous detection and classification of region proposals and a new incremental action tube generation approach, our method achieves superior performances compared to the previous state-of-the-art on early action prediction and on-line localisation, while outperforming the top offline competitors on UCF-101, in particular at high detection overlap. Its combination of high accuracy and fast detection speed at test time paves the way for its application to real-time applications such as autonomous driving, human robot interaction and surgical robotics, among others.

References

- [1] T. Brox, A. Bruhn, N. Papenberg, and J. Weickert. High accuracy optical flow estimation based on a theory for warping. 2004. [2](#), [3](#), [4](#), [6](#)
- [2] R. De Geest, E. Gavves, A. Ghodrati, Z. Li, C. Snoek, and T. Tuytelaars. Online action detection. *arXiv preprint arXiv:1604.06506*, 2016. [3](#), [4](#)
- [3] G. Evangelidis, G. Singh, and R. Horaud. Continuous gesture recognition from articulated poses. In *ECCV Workshops*, 2014. [3](#), [5](#)
- [4] A. Gaidon, Z. Harchaoui, and C. Schmid. Temporal localization of actions with actoms. *Pattern Analysis and Machine Intelligence, IEEE Transactions on*, 35(11):2782–2795, 2013. [3](#)
- [5] R. Girshick, J. Donahue, T. Darrel, and J. Malik. Rich feature hierarchies for accurate object detection and semantic segmentation. In *IEEE Int. Conf. on Computer Vision and Pattern Recognition*, 2014. [2](#), [3](#)
- [6] G. Gkioxari and J. Malik. Finding action tubes. In *IEEE Int. Conf. on Computer Vision and Pattern Recognition*, 2015. [2](#), [3](#), [4](#), [5](#), [8](#)
- [7] M. Hoai and F. De la Torre. Max-margin early event detectors. *International Journal of Computer Vision*, 107(2):191–202, 2014. [4](#)
- [8] M. Jain, J. Van Gemert, H. Jégou, P. Bouthemy, and C. G. Snoek. Action localization with tubelets from motion. In *Computer Vision and Pattern Recognition (CVPR), 2014 IEEE Conference on*, pages 740–747. IEEE, 2014. [3](#)
- [9] S. D. Jain and K. Grauman. Supervoxel-consistent foreground propagation in video. In *Computer Vision–ECCV 2014*, pages 656–671. Springer, 2014. [3](#)
- [10] H. Jhuang, J. Gall, S. Zuffi, C. Schmid, and M. Black. Towards understanding action recognition. 2013. [6](#)
- [11] S. Ji, W. Xu, M. Yang, and K. Yu. 3d convolutional neural networks for human action recognition. *Pattern Analysis and Machine Intelligence, IEEE Transactions on*, 35(1):221–231, Jan 2013. [3](#)
- [12] A. Karpathy, G. Toderici, S. Shetty, T. Leung, R. Sukthankar, and L. Fei-Fei. Large-scale video classification with convolutional neural networks. In *IEEE Int. Conf. on Computer Vision and Pattern Recognition*, 2014. [3](#)
- [13] A. Krizhevsky, I. Sutskever, and G. E. Hinton. Imagenet classification with deep convolutional neural networks. In *Advances in Neural Information Processing Systems*, 2012. [2](#)
- [14] T. Kroeger, R. Timofte, D. Dai, and L. Van Gool. Fast optical flow using dense inverse search. *arXiv preprint arXiv:1603.03590*, 2016. [2](#), [3](#), [4](#), [6](#), [8](#)
- [15] H. Kuehne, H. Jhuang, E. Garrote, T. Poggio, and T. Serre. Hmdb: a large video database for human motion recognition. In *Computer Vision (ICCV), 2011 IEEE International Conference on*, pages 2556–2563. IEEE, 2011. [6](#)
- [16] K. Kulkarni, G. Evangelidis, J. Cech, and R. Horaud. Continuous action recognition based on sequence alignment. *International Journal of Computer Vision*, 112(1):90–114, 2015. [3](#)
- [17] T. Lan, T.-C. Chen, and S. Savarese. A hierarchical representation for future action prediction. In *Computer Vision–ECCV 2014*, pages 689–704. Springer, 2014. [4](#)
- [18] I. Laptev and P. Pérez. Retrieving actions in movies. In *Computer Vision, 2007. ICCV 2007. IEEE 11th International Conference on*, pages 1–8. IEEE, 2007. [3](#)
- [19] T.-Y. Lin, M. Maire, S. Belongie, J. Hays, P. Perona, D. Ramanan, P. Dollár, and C. L. Zitnick. Microsoft coco: Common objects in context. In *European Conference on Computer Vision*, pages 740–755. Springer, 2014. [7](#)
- [20] W. Liu, D. Anguelov, D. Erhan, C. Szegedy, S. Reed, C.-Y. Fu, and A. C. Berg. SSD: Single shot multibox detector. *arXiv preprint arXiv:1512.02325*, 2015. [2](#), [3](#), [4](#)
- [21] J. Lu, r. Xu, and J. J. Corso. Human action segmentation with hierarchical supervoxel consistency. In *IEEE Int. Conf. on Computer Vision and Pattern Recognition*, June 2015. [3](#)
- [22] B. Majecka. Statistical models of pedestrian behaviour in the forum. *Master’s thesis, School of Informatics, University of Edinburgh*, 2009. [5](#)
- [23] A. Milan, K. Schindler, and S. Roth. Multi-target tracking by discrete-continuous energy minimization. *IEEE TPAMI*, 2016. [5](#)
- [24] D. Oneata, J. Verbeek, and C. Schmid. Efficient action localization with approximately normalized fisher vectors. In *Proceedings of the IEEE Conference on Computer Vision and Pattern Recognition*, pages 2545–2552, 2014. [3](#)

- [25] X. Peng and C. Schmid. Multi-region two-stream R-CNN for action detection. In *ECCV 2016 - European Conference on Computer Vision*, Amsterdam, Netherlands, Oct. 2016. 1, 2, 3, 4, 6, 7, 8
- [26] S. Ren, K. He, R. Girshick, and J. Sun. Faster R-CNN: Towards real-time object detection with region proposal networks. In *Advances in Neural Information Processing Systems*, pages 91–99, 2015. 2, 4
- [27] M. Ryoo. Human activity prediction: Early recognition of ongoing activities from streaming videos. In *Computer Vision (ICCV), 2011 IEEE International Conference on*, pages 1036–1043. IEEE, 2011. 4
- [28] M. S. Ryoo and J. Aggarwal. Ut-interaction dataset, icpr contest on semantic description of human activities (sdha). In *IEEE International Conference on Pattern Recognition Workshops*, volume 2, page 4, 2010. 4
- [29] S. Saha, G. Singh, M. Sapienza, P. H. S. Torr, and F. Cuzzolin. Deep learning for detecting multiple space-time action tubes in videos. In *British Machine Vision Conference*, 2016. 1, 2, 3, 4, 5, 6, 7, 8
- [30] M. Sapienza, F. Cuzzolin, and P. H. Torr. Learning discriminative space-time action parts from weakly labelled videos. *Int. Journal of Computer Vision*, 2014. 3
- [31] C. Schödl, I. Laptev, and B. Caputo. Recognizing human actions: a local svm approach. In *Pattern Recognition, 2004. ICPR 2004. Proceedings of the 17th International Conference on*, volume 3, pages 32–36. IEEE, 2004. 4
- [32] Z. Shou, D. Wang, and S. Chang. Action temporal localization in untrimmed videos via multi-stage cnns. In *IEEE Int. Conf. on Computer Vision and Pattern Recognition*, June 2016. 3
- [33] K. Simonyan and A. Zisserman. Two-stream convolutional networks for action recognition in videos. In *Advances in Neural Information Processing Systems 27*, pages 568–576. Curran Associates, Inc., 2014. 3, 4
- [34] B. Singh and M. Shao. A multi-stream bi-directional recurrent neural network for fine-grained action detection. In *IEEE Int. Conf. on Computer Vision and Pattern Recognition*, 2016. 3
- [35] G. Singh. Categorising the abnormal behaviour from an indoor overhead camera. *Bachelor's thesis, VIT University*, 2010. 5
- [36] G. Singh and F. Cuzzolin. Untrimmed video classification for activity detection: submission to activitynet challenge. *arXiv preprint arXiv:1607.01979*, 2016. 3
- [37] K. Soomro, H. Idrees, and M. Shah. Action localization in videos through context walk. In *Proceedings of the IEEE International Conference on Computer Vision*, 2015. 3
- [38] K. Soomro, H. Idrees, and M. Shah. Predicting the where and what of actors and actions through online action localization. 2016. 2, 3, 4, 6, 7
- [39] K. Soomro, A. R. Zamir, and M. Shah. UCF101: A dataset of 101 human action classes from videos in the wild. Technical report, CRCV-TR-12-01, 2012. 1, 6
- [40] R. Šrámek, B. Brejová, and T. Vinař. On-line viterbi algorithm and its relationship to random walks. *arXiv preprint arXiv:0704.0062*, 2007. 5
- [41] W. Sultani and M. Shah. What if we do not have multiple videos of the same action? - video action localization using web images. In *IEEE Int. Conf. on Computer Vision and Pattern Recognition*, 2016. 3
- [42] Y. Tian, R. Sukthankar, and M. Shah. Spatiotemporal deformable part models for action detection. In *Computer Vision and Pattern Recognition (CVPR), 2013 IEEE Conference on*, pages 2642–2649. IEEE, 2013. 3
- [43] D. Tran, L. Bourdev, R. Fergus, L. Torresani, and M. Paluri. Learning spatiotemporal features with 3d convolutional networks. *Proc. Int. Conf. Computer Vision*, 2015. 3
- [44] J. Uijlings, K. van de Sande, T. Gevers, and A. Smeulders. Selective search for object recognition. *Int. Journal of Computer Vision*, 2013. 2
- [45] J. C. van Gemert, M. Jain, E. Gati, and C. G. Snoek. APT: Action localization proposals from dense trajectories. In *BMVC*, volume 2, page 4, 2015. 3, 6
- [46] H. Wang, A. Kläser, C. Schmid, and C. Liu. Action Recognition by Dense Trajectories. In *IEEE Int. Conf. on Computer Vision and Pattern Recognition*, 2011. 3
- [47] H. Wang, D. Oneata, J. Verbeek, and C. Schmid. A robust and efficient video representation for action recognition. *International Journal of Computer Vision*, pages 1–20, 2015. 3
- [48] L. Wang, Y. Qiao, X. Tang, and L. Van Gool. Actionness estimation using hybrid fully convolutional networks. *IEEE Int. Conf. on Computer Vision and Pattern Recognition*, 2016. 3, 8
- [49] P. Weinzaepfel, Z. Harchaoui, and C. Schmid. Learning to track for spatio-temporal action localization. In *IEEE Int. Conf. on Computer Vision and Pattern Recognition*, June 2015. 1, 2, 3, 4, 6, 7, 8
- [50] P. Weinzaepfel, X. Martin, and C. Schmid. Towards weakly-supervised action localization. *arXiv preprint arXiv:1605.05197*, 2016. 3
- [51] Z. Xu, Y. Yang, and A. G. Hauptmann. A discriminative cnn video representation for event detection. *arXiv preprint arXiv:1411.4006*, 2014. 3
- [52] S. Yeung, O. Russakovsky, N. Jin, M. Andriluka, G. Mori, and L. Fei-Fei. Every moment counts: Dense detailed labeling of actions in complex videos. *arXiv preprint arXiv:1507.05738*, 2015. 3
- [53] S. Yeung, O. Russakovsky, G. Mori, and L. Fei-Fei. End-to-end learning of action detection from frame glimpses in videos. *CVPR*, 2016. 3
- [54] G. Yu and J. Yuan. Fast action proposals for human action detection and search. In *Proceedings of the IEEE Conference on Computer Vision and Pattern Recognition*, pages 1302–1311, 2015. 6, 7, 8
- [55] T.-H. Yu, T.-K. Kim, and R. Cipolla. Real-time action recognition by spatiotemporal semantic and structural forests. In *BMVC*, volume 2, page 6, 2010. 4
- [56] B. Zhang, L. Wang, Z. Wang, Y. Qiao, and H. Wang. Real-time action recognition with enhanced motion vector cnns. *CVPR*, 2016. 4
- [57] C. L. Zitnick and P. Dollár. Edge boxes: Locating object proposals from edges. In *Computer Vision—ECCV 2014*, pages 391–405. Springer, 2014. 2, 4